The comparison of $SrTi_{0.98}Nb_{0.02}O_{3-\delta}$-$CeO_2$ and $SrTi_{0.98}Nb_{0.02}O_{3-\delta}$-YSZ composites for use in SOFC anodes

B. Bochentyn · J. Karczewski · S. Molin · T. Klimczuk ·
M. Gazda · P. Jasinski · D. J. Safarik · B. Kusz

Abstract Composites of Nb-doped strontium titanate mixed with yttria-stabilized zirconia or cerium oxide in 50:50, 70:30 and 85:15 weight ratios were evaluated as possible anode/electrolyte interface materials for solid oxide fuel cells in terms of chemical compatibility, electrical conductivity and mechanical properties. It has been shown that composite samples prepared by typical powder-mixing methods remain single-phase up to 1400°C. The electrical conductivity of these composites, regardless of their composition and fabrication conditions, is lower than the conductivity of pure $SrTi_{0.98}Nb_{0.02}O_{3-\delta}$, but in most cases sufficient for solid oxide fuel cells anode application. The best properties are found for samples reduced at 1400°C for 10 h in H_2 atmosphere. The observations made by scanning electron microscope suggest that the grains of both phases are well-distributed throughout the whole volume of the investigated samples, and that the composites with CeO_2 better adhere to the electrolyte surface. The electrical results confirm that composites with at most 30 wt % of YSZ/CeO_2 phase fulfill the anode requirements. However, the fuel cell performance tests indicate that the application of composite with CeO_2 results in the lower power density than the application of the composite with YSZ.

Keywords Solid oxide fuel cell · Nb-doped $SrTiO_3$ · Anode · Composite

1 Introduction

The dominant anode material for Solid Oxide Fuel Cell (SOFC) application is a Ni-YSZ (metallic-ceramic) composite of Ni and yttria-stabilized zirconia (YSZ). The cermet has many advantages, such as high catalytic activity, thermal expansion coefficient (TEC) compatible with the electrolyte (YSZ) [1] and high value of electrical conductivity [2]. However, it is also sensitive to deposition of carbon on the surface, which blocks the anode reaction, and can be poisoned by sulphur [2, 3]. These problems limit the possibility of using Ni-YSZ for carbon-containing fuels. Moreover, Ni-YSZ can undergo microstructural changes during redox cycles, which can reduce the three-phase area and thereby reduce the electrode activity [2, 3].

There is a strong need to find an alternative to Ni-YSZ cermets for SOFC applications. The most promising materials are perovskite-related structures, such as $SrTiO_3$. Substitution of a rare earth element (e.g. yttrium) into the A sublattice of $SrTiO_3$, or a transition metal (e.g. niobium) into the B sublattice, increases the electronic conductivity of the material [4, 5]. It has been shown recently that the samples in which 2% of

B. Bochentyn (✉) · J. Karczewski · T. Klimczuk · M. Gazda ·
B. Kusz
Faculty of Applied Physics and Mathematics,
Gdansk University of Technology,
ul. Narutowicza 11/12,
80-233 Gdansk, Poland
e-mail: bbochentyn@mif.pg.gda.pl

S. Molin · P. Jasinski
Faculty of Electronics, Telecommunication and Informatics,
Gdansk University of Technology,
ul. Narutowicza 11/12,
80-233 Gdansk, Poland

T. Klimczuk
European Commission, Joint Research Center,
Institute for Transuranium Elements,
Postfach 2340,
Karlsruhe D-76125, Germany

D. J. Safarik
Los Alamos National Laboratory,
Los Alamos, NM 87545, USA

titanium is substituted with niobium: $SrTi_{0.98}Nb_{0.02}O_{3-\delta}$ (STNb2) have the highest conductivity in comparison with the other investigated compositions [5]. The conductivity of strontium titanate may also be increased by introducing the strontium vacancies [6] and by annealing the material in reducing conditions (e.g. the NH_3 atmosphere) [7]. Due to its high electronic conductivity, doped $SrTiO_3$ may be competitive to Ni-YSZ as a SOFC anode material. However, at present the ionic conductivity and the catalytic properties of $SrTiO_3$ are not sufficient for anode application [8]. Moreover, the $SrTiO_3$ anode tends to delaminate from the electrolyte surface [9, 10].

The aim of this work is to eliminate these limitations. The idea is based on an analogy to Ni-YSZ anodes. The high temperature firing of the nickel cermet allows the YSZ phase from the anode composite to sinter with the YSZ electrolyte. As a result, a seamless interface between the anode and the electrolyte is formed, and channels, which allow ionic conduction into the electrode, are created [11]. In the case of perovskites, the composite of perovskite phase and YSZ applied as an interface layer is expected to reduce the delamination processes and increase the triple phase boundary (TPB). In consequence, it should improve the mechanical stability of the anode/electrolyte interface and may result in the increase of fuel cell performance.

Another possible composite material for use at the anode/electrolyte interface is a doped-$SrTiO_3$/cerium oxide or doped-$SrTiO_3$/gadolinia-doped ceria (CGO), in which ceria offers the dual benefits of conductivity and catalytic activity. Both doped and undoped ceria are mixed ionic and electronic conductors at low oxygen partial pressure. CeO_{2-x} has high values of oxygen surface exchange and presents an n-type conductivity of about 1 S/cm at 900°C in oxygen partial pressure of 10^{-18} atm [8]. In this paper only results obtained for undoped ceria will be presented in order to avoid additional complications from possible reactions between Gd_2O_3 and $SrTiO_3$ phases. Moreover, pure CeO_2 seems to fulfil necessary requirements of ionically conducting component of composite.

There are various methods of composite preparation. Samples produced by a typical mixing powders method present both mechanical and electrical advantages. However, Ahn et al. [10] suggest that the process of YSZ / CeO_2 impregnation with STNb2, instead of mixing powders, will provide sufficient electronic conductivity even if conductive phase is lower than 30-vol%. They observed that a non-random structure is formed in which the electronically conductive component (STNb2) coats the YSZ / CeO_2 backbone. On the other hand, it is reported [10] that it is difficult to produce mechanically strong composites based on the porous YSZ / CeO_2.

In this paper the properties of the composites of $SrTi_{0.98}Nb_{0.02}O_{3-\delta}$ with YSZ or CeO_2, prepared by mixing powder method, will be presented and discussed. The possibility of using these composites at the SOFC anode/electrolyte interface has been examined.

2 Experimental

Composites of $xSrTi_{0.98}Nb_{0.02}O_{3-\delta}$-$(100-x)CeO_2$ (STNb2-CeO_2) and $xSrTi_{0.98}Nb_{0.02}O_{3-\delta}$-$(100-x)YSZ$ (STNb2-YSZ) (where x=50,70,85 wt. % of STNb2) were fabricated at various temperatures of calcination (1200–1400°C) and reduction (1200–1400°C) in hydrogen for up to 10 h. The 50, 70 and 85 weight % of STNb2 correspond to 58, 77 and 89 vol.% of STNb2 in the case of STNb2-CeO_2 composites, whereas in the case of STNb2-YSZ composites such weight ratios correspond to 54, 73 and 87 vol. % of STNb2, respectively.

The $SrTi_{0.98}Nb_{0.02}O_{3-\delta}$ ceramic was prepared using a conventional solid-state reaction method. $SrCO_3$ (Sigma Aldrich), TiO_2 (Sigma Aldrich) and Nb_2O_5 (Fluka) powders were mixed in the suitable stoichiometric ratios and ball milled with ethanol for 24 h. After drying the mixture was pressed into bars (~280 MPa) and calcined in air at 1200°C for 12 h. Then, the pellets were reground to obtain better samples quality, uniaxially pressed at 560 MPa and sintered at 1400°C for 12 h in air. The $SrTi_{0.98}Nb_{0.02}O_{3-\delta}$ samples prepared in this way were ball milled again to obtain a fine-grained anode powder. Then the powder was mixed in a proper weight ratio either with YSZ (8-mol% yttria-stabilized zirconia, Daiichi Kigenso HSY-8) or with CeO_2 (Fluka) powder in a ball mill for 12 h. This final ball-milling step is necessary to disperse the two phases of the composite. Indeed, we find that if we use a mortar, rather than the ball mill, the grains of electronically conductive (STNb2) phase agglomerate, creating large islands that are isolated from each other. To obtain porous samples the composite powder was mixed with starch (5 wt. %).

To improve the electrical properties all of the samples after the synthesis were reduced in dry hydrogen at various temperatures (1200°C–1400°C). For comparison, some samples of each composition, before the reduction, were sintered at 1400°C for 3 h in air. Such processes of initial heat treatment in air strongly influence the porosity. The values of porosity vary in the range of 10% to 35% and are presented together with the conductivity plots in the further part of this paper. The thickness of the bulk samples was approximately 1 mm, while of the thin layers was approximately 50 μm.

To examine the materials in the operating fuel cell the powders were mixed with 5 wt % of carbon black and the organic binder. One layer of composite paste (approximately 15 μm thick) and 2 layers of STNb2 anode paste (approximately 30 μm thick) were painted onto the surface of dense

0.8 mm thick YSZ electrolyte. In order to burn out the organic binder, the cells were calcined at 700°C for 3 h in air. Then they were reduced at 1400°C for 10 h in dry hydrogen. Finally, the La(Ni,Fe)O$_3$ cathode material was deposited on the cells. Cathode was sintered during the operation of the cell. All the cell measurements were taken at 800°C using humidified (3% H$_2$0) hydrogen as a fuel and air as an oxidant.

The composites were examined using various methods. The phase composition of the bulk samples was analyzed by an X-ray diffraction method by the X'Pert Pro MPD Philips diffractometer using Cu K$_\alpha$ (1.542 Å) radiation at room temperature. The electrical conductivity of bulk samples was measured using the four terminal DC method over temperature range of 400–950°C in humidified hydrogen. The measurements were performed at constant heating and cooling rates (2°C/min) on bar samples with parallel 9907 ESL silver electrodes. The current–voltage (i-V) curves of operating fuel cells were obtained by a Solartron 1260 Frequency Response Analyzer coupled with Solartron 1294 Impedance Interface. The morphology of the samples was characterized by the Philips XL30 scanning electron microscope (SEM), using secondary electron (SE) and back-scattered electron (BSE) detectors. To recognize the elements and their distribution in composite samples the Energy-Dispersive X-ray spectroscopy (EDX) was performed by the EDAX Sapphire® spectrometer in particular points of each sample. The density of the samples was measured with the Archimedes method assisted by vacuum saturation.

3 Results and discussion

The results of XRD analysis for the xSTNb2-(100-x)YSZ and xSTNb2-(100-x)CeO$_2$ (where x=50,70,85 wt. % of STNb2) composite powders are presented in Figs. 1 and 2 respectively. All of the reflections observed in XRD patterns can be attributed to either strontium titanate or YSZ / CeO$_2$ phases. Thus, there appears to be a little, if any, chemical reaction between STNb2 and YSZ or CeO$_2$, regardless of the composition and the heat treatment conditions. A small change in intensity of the CeO$_2$ peaks relative to those of STNb2 has been observed after a reduction of composite sample. However, Ma et al. reports in their recent work [11], that there is a diffusion of Ti from SrTiO$_3$ anode to the YSZ electrolyte layer in the operating fuel cell system. Although no impurity peaks are observed in the XRD results, this phenomenon also takes place to a slight extent between the components of the STNb2-YSZ composite, what was confirmed by the EDX analysis in our work.

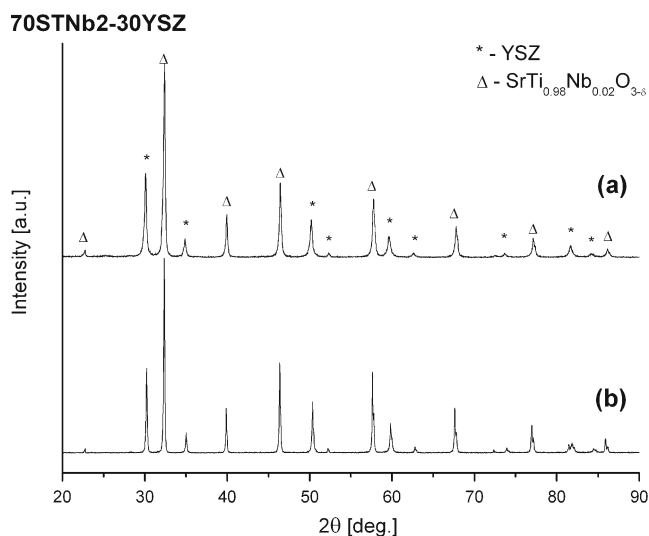Figures 3 and 4 show the SEM images of the surface of STNb2-CeO$_2$ and STNb2-YSZ composites that were

Fig. 1 XRD pattern of a composite with 70-wt % STNb2 and 30-wt % of YSZ (70STNb2–30YSZ): (**a**) before heat treatment, (**b**) reduced at 1400°C for 10 h in H$_2$

reduced in H$_2$ at 1400°C for 10 h. For both types of composites, the darker grains in back-scattering images refer to the SrTi$_{0.98}$Nb$_{0.02}$O$_{3-\delta}$ phase. It can be observed that the STNb2 and CeO$_2$ / YSZ grains are well distributed in the analyzed composites. The surface occupied by CeO$_2$ / YSZ grains in the images corresponds well with the volume fraction of CeO$_2$ / YSZ in composites. The average grain size of CeO$_2$ is 2–3 μm, whereas the grain size of YSZ is approximately 1–2 μm. However, it should be noticed, that the shape of CeO$_2$ grains is elongated while that of the YSZ is round. Such phenomenon is very interesting and requires further investigation to explain the observed differences in the shape of grains.
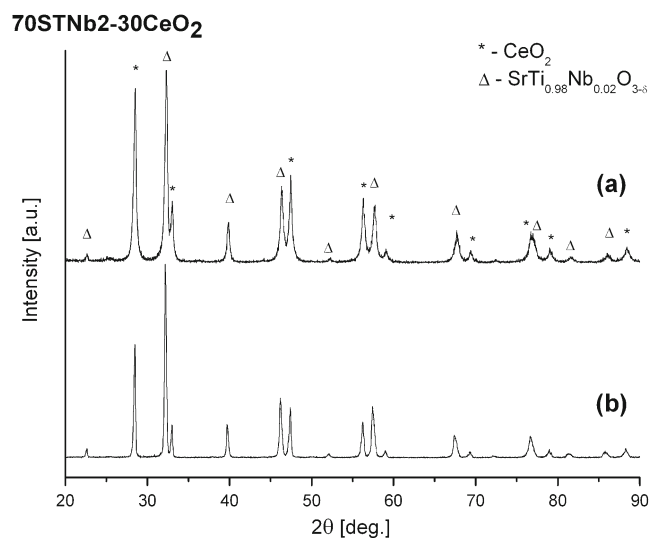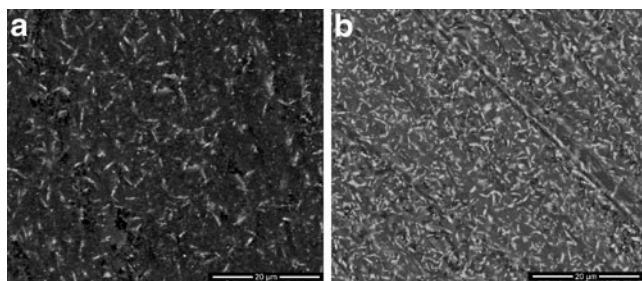

Fig. 2 XRD pattern of a composite with 70-wt % STNb2 and 30-wt % of CeO$_2$ (70STNb2–30CeO$_2$): (**a**) before heat treatment, (**b**) reduced at 1400°C for 10 h in H$_2$

Fig. 3 SEM images showing the polished surface of (**a**) 85STNb2–15CeO$_2$, (**b**) 70STNb2–30CeO$_2$ samples made by the backscattered electron detector (BSE)

The SEM observations also suggest that the phase distribution is not influenced by heat treatment. It appears that the heat treatment changes only the density of the samples. Specifically, density increases with the temperature of initial calcination / reduction.

The cross-sectional images of the STNb2/STNb2-YSZ/YSZ and STNb2/STNb2-CeO$_2$/YSZ interfaces, presented in Fig. 5(a) and (b), show that both composite layers show quite homogenous porosity, but STNb2-YSZ grains and pores seem to be smaller and better distributed. Moreover, the STNb2-CeO$_2$ composite adheres better to the YSZ electrolyte than the STNb2-YSZ composite. Our observation of a tight junction at the STNb2-CeO$_2$/YSZ interface corresponds well with the observations of Sun et al. [12, 13]. They report that the addition of CeO$_2$ can decrease the mismatch between the anode and electrolyte. It should be also noticed that a kind of dense layer at the anode/electrolyte interface is created. The result of EDX analysis of this layer, presented in Fig. 6, shows that this layer consists of YSZ electrolyte, to which some amount of Ce and Ti has diffused. In the following parts of this paper the acronym YSZ (Ce,Ti) will be used to describe this layer.

Results of electrical conductivity measurements of composites containing 15 wt. % of YSZ and heat-treated under various conditions are presented in Fig. 7. It is very important for anode materials to have sufficient electrical conductivity in the fuel cell operating environment. Tao and Irvine

[14] reported that the minimum conductivity required to minimize the SOFC anode ohmic losses is about 1S/cm. Our results show that, regardless of composition and initial heat treatment, it is necessary to reduce the composites at ≥1300°C to achieve 1 S/cm. As presented in Fig. 7, the highest conductivity was achieved for samples reduced at 1400°C for 10 h in H$_2$ atmosphere. These samples are hard, do not crack and are chemically stable during the processes of heating and cooling, so only materials prepared in this way will be analyzed in the following parts of this paper. It was observed that the process of initial calcination does not improve the conductivity of the material significantly. There is even a slight deterioration of electrical properties. The initial calcination may moderate the process of reduction, which might explain the observed differences.

One of the most important aims of this work was to prepare the material presenting high electronic conductivity with the simultaneously higher ionic conductivity than that of the pure SrTiO$_3$ material. The electrical conductivity results for composites with various STNb2:YSZ and STNb2:CeO$_2$ weight ratios are compared in Figs. 8 and 9. For all composites investigated in this work, a thermally activated behaviour is observed. As expected, the highest total conductivity in the whole temperature range is shown by 85STNb2–15YSZ composition. The conductivity of materials with 30 wt. % of YSZ is slightly lower, but also sufficient for use in fuel cells. It should be noticed that the conductivity level of composites with about 15 wt. % of YSZ is comparable to the conductivity of pure STNb2 sample with about 11% porosity reported by Karczewski et al. [5]. In the case of 50STNb2–50YSZ, the concentration of electronically conductive phase (STNb2) is low and there seems to be no percolation path (Fig. 4(c)). This limits the efficient transport of charge carriers, and thus explains the low value of conductivity (Fig. 8).

For the STNb2-CeO$_2$ composites (Fig. 9), in which the addition of CeO$_2$ phase was to improve the catalytic properties of the material, the same tendency is observed. However, the conductivity of the 85STNb2–15CeO$_2$ sample is considerably higher than that of 70STNb2–30CeO$_2$.
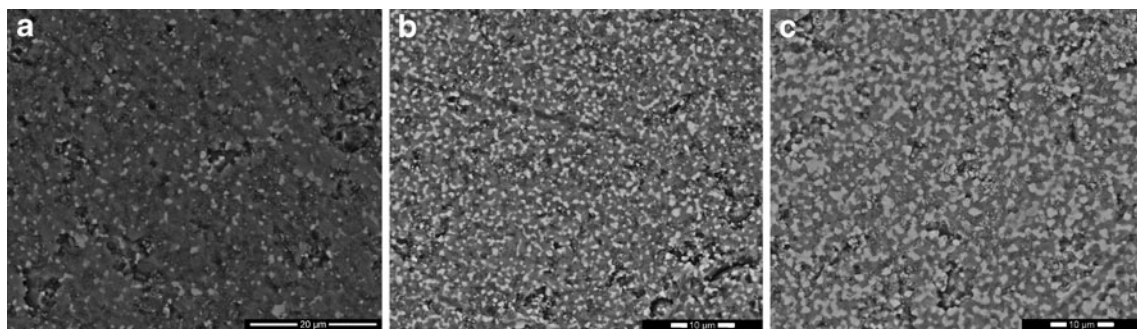

Fig. 4 SEM images showing the polished surface of (**a**) 85STNb2–15YSZ, (**b**) 70STNb2–30YSZ, (**c**) 50STNb2–50YSZ samples made by the backscattered electron detector (BSE)

Fig. 5 SEM images showing the cross section of fuel cells' fragments with composite (**a**) 70STNb2–30YSZ or (**b**) 70STNb2–30CeO$_2$ layers made by the secondary electron (SE) detector. The boundary between layers was specified on the basis of EDX measurements
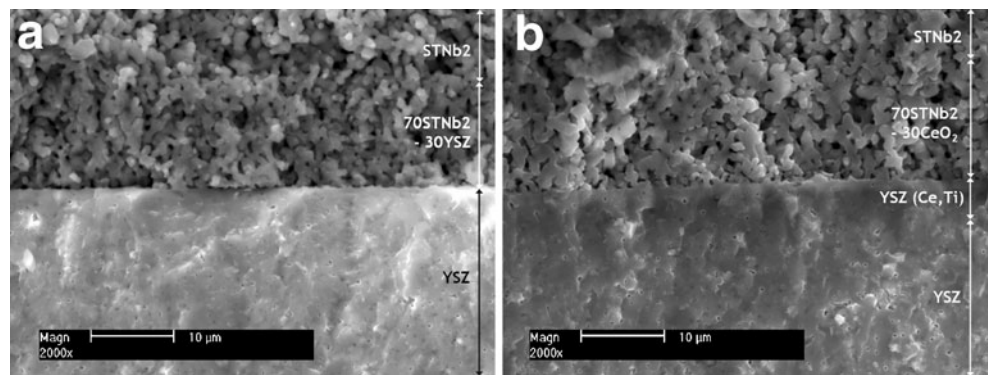
The comparison of electrical conductivity plots for composite bulk samples reduced at 1400°C for 10 h in H$_2$ atmosphere is presented in Fig. 10. The conductivity of both 85STNb2–15YSZ and 85STNb2–15CeO$_2$ in the SOFC operating temperature range is relatively high, but the temperature dependence of the conductivity is different for these two materials. It has been reported that at high temperature and in reducing conditions, the electronic component of conductivity in CeO$_2$ starts to play a significant role in total conductivity of the composite. This agrees with the rapid increase of conductivity of 85STNb2–15CeO$_2$ in comparison to 85STNb2–15YSZ material (Fig. 10).

The cell voltage and power density plots as a function of current density obtained for fuel cells operating at 800°C are shown in Fig. 11. Three types of anodes: pure STNb2, 70STNb2–30YSZ composite and 70STNb2–30CeO$_2$ respectively, have been examined. The open circuit voltage (OCV) of all cells is about 1.07 V and is close to the theoretical one predicted using the Nernst equation. The highest power density was obtained by the fuel cell with a STNb2-YSZ composite as an anode. It can be caused by the

triple phase boundary extension with reference to pure STNb2. For comparison, the composite with CeO$_2$ as an anode causes the power density decrease relative to that of pure STNb2 anode. We suggest that this deterioration can result from the dense YSZ (Ce,Ti) layer creation, which was reported in the previous part of this paper. Although no negative effects have been noticed in the electrical results of STNb2-CeO$_2$ composite, the YSZ (Ce,Ti) layer, forming between the composite and electrolyte, can be responsible for the contraction of triple phase boundary in the operating fuel cell. In consequence, the performance of a fuel cell decreases.

In order to mix the advantages of both STNb2-YSZ and STNb2-CeO$_2$ composites there is an idea to infiltrate the STNb2 or STNb2-YSZ anode support with CeO$_2$ solution instead of mixing powders. Such process may prevent the creation of YSZ (Ce,Ti) dense layer responsible for the fuel cell performance's decrease and should be investigated further.

It should be also noticed that a higher cell performance for all samples is expected when reducing the thickness of

Fig. 6 EDX spectrum of a dense layer created between the STNb2-CeO$_2$ composite and the YSZ electrolyte. The Cu presence in the spectrum reflects the sample support used in the EDX equipment
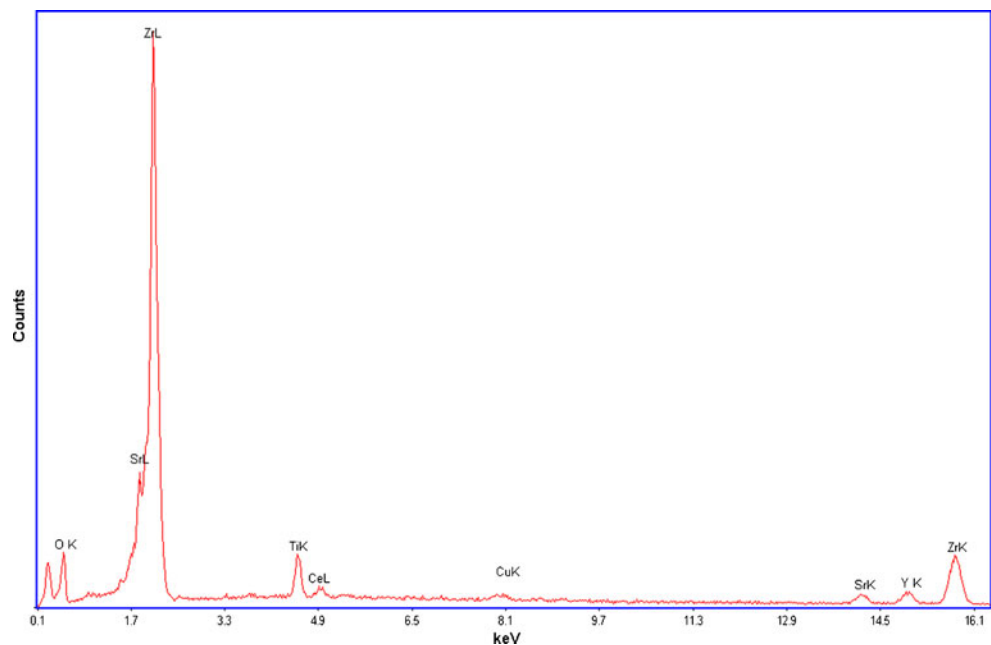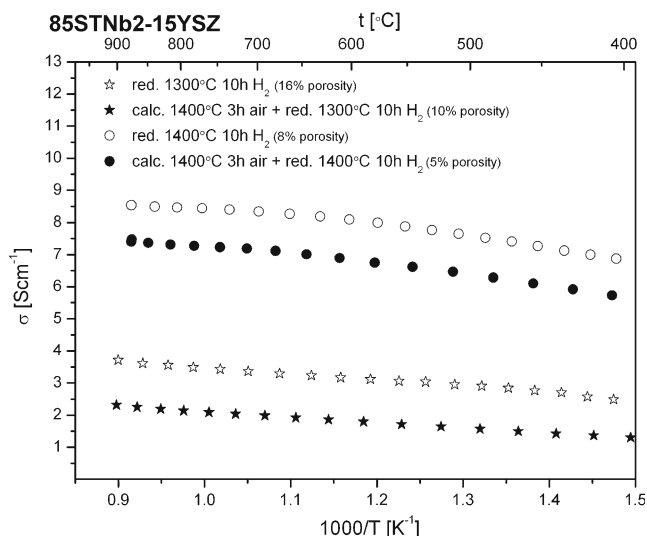
Fig. 7 Electrical conductivity plots of 85STNb2–15YSZ bulk samples heat-treated in various conditions as a function of temperature

Fig. 9 Electrical conductivity plots of STNb2-CeO$_2$ bulk samples reduced at 1400°C for 10 h in H$_2$ as a function of temperature

the electrolyte and using better cathode material. Moreover, the catalytic activity of anode can be additionally increased by infiltrating it with small amounts of a catalyst, such as Ce, Ni, Co, Ru, Pt and Pd. These catalysts decrease the polarisation resistance of anode and some of them (e.g. Ce, Ru) improve the anode tolerance to sulphur containing fuels [15, 16].

Another fact that should be considered, is the mechanical misfit between the composite components. This appears to be especially important for STNb2-CeO$_2$, because the resistance to layer cracking and delamination during reduction-oxidation decreases with the increasing CeO$_2$ concentration [8, 12]. Koutcheiko et al. [8] reports that it is caused by the
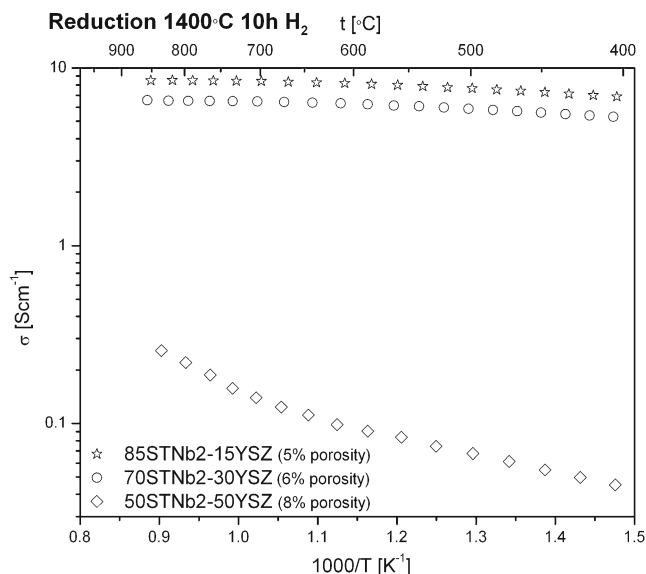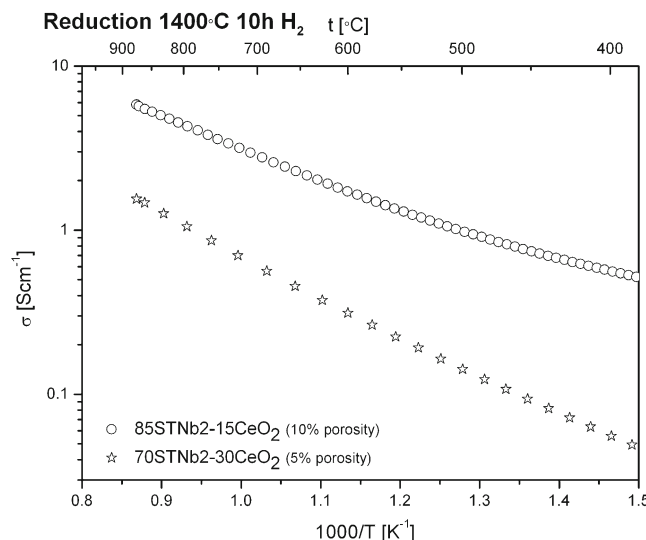
contraction of the CeO$_2$ lattice parameter in less reducing atmospheres. The thermal expansion coefficient (TEC) of composites consisting of yttrium-doped strontium titanate and cerium oxide is very similar to the TEC of YSZ (10.3 × 10^{-6} K^{-1} [8, 17]), at least in the temperature range 50–1000°C and in air [8]. However, the value of the TEC increases in a reducing atmosphere, and the higher the concentration of CeO$_2$ in the composite, the higher the TEC of composite material [8]. We observed, in the present work, that this mismatch results in the cracking of bulk pellets and in the delamination of composite layers from the YSZ electrolyte support. Mixing with starch to increase porosity minimizes this problem for samples with 15 and 30 wt. % of CeO$_2$.
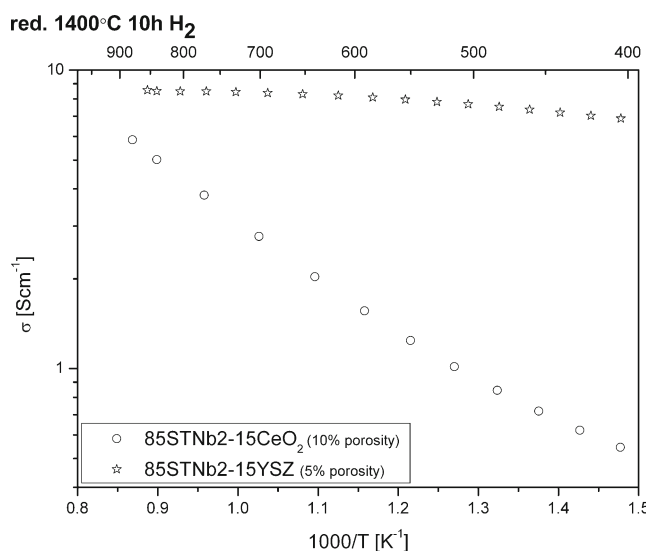

Fig. 8 Electrical conductivity plots of STNb2-YSZ bulk samples reduced at 1400°C for 10 h in H$_2$ as a function of temperature

Fig. 10 The comparison of electrical conductivity plots of 85STNb2–15YSZ and 85STNb2–15CeO$_2$ bulk samples reduced at 1400°C for 10 h in H$_2$ as a function of temperature
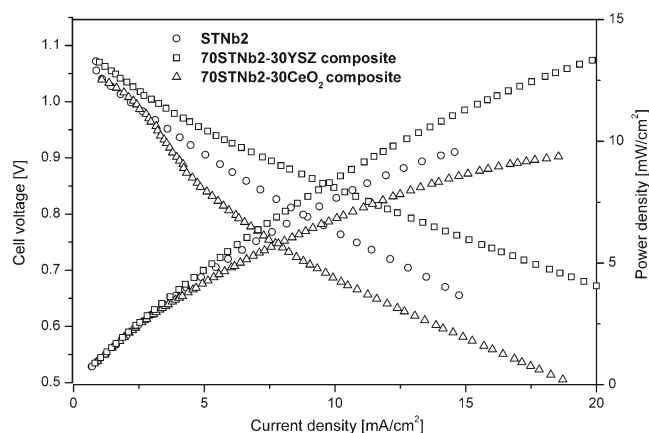
Fig. 11 I-V and power density plots for fuel cells with various anodes operating at 800°C in humidified H_2

However, even with the increased porosity, composites with 50 wt. % of CeO_2 are still mechanically unstable and not suitable for SOFC application. The problems with TEC misfit between the composite and the YSZ electrolyte do not take place for STNb2-YSZ.

4 Conclusion

The electrical and structural properties of $xSrTi_{0.98}Nb_{0.02}O_{3-\delta}$-(100-x)$CeO_2$ and $xSrTi_{0.98}Nb_{0.02}O_{3-\delta}$-(100-x)YSZ (where x=50,70,85 wt. % of $SrTi_{0.98}Nb_{0.02}O_{3-\delta}$) have been studied, with particular attention given to their potential for use at anode/electrolyte interfaces in SOFC. The XRD analyses demonstrate, that in all investigated composites there is no reaction between the components. The required conductivity level is obtained for at least 70 weight % of perovskite phase content. The best properties were observed for samples reduced at 1400°C for 10 h in H_2 atmosphere. The SEM analysis confirms a good dispersion of both phases in the investigated composites. Although the STNb2-CeO_2 composite material (with at most 30 wt. % of CeO_2) presents very good

References

1. J.W. Fergus, Solid State Ionics **177**, 1529–1541 (2006)
2. W.Z. Zhu, S.C. Deevi, Mater Sci Eng **A362**, 228–239 (2003)
3. Y. Matsuzaki, I. Yasuda, Solid State Ionics **132**, 261–269 (2000)
4. T. Kolodiazhnyi, A. Petric, Journal of Electroceramics **15**, 5–11 (2005)
5. J. Karczewski, B. Riegel, M. Gazda, P. Jasinski, B. Kusz, Journal of Electroceramics **24**, 326–330 (2010)
6. S. Hui, A. Petric, J Electrochem Soc **149**(1), J1–J10 (2002)
7. J. Karczewski, B. Riegel, S. Molin, M. Gazda, P. Jasinski, L. Murawski, B. Kusz, J Alloys Compd **473**, 496–499 (2009)
8. S. Koutcheiko, Y. Yoo, A. Petric, I. Davidson, Ceram Int **32**, 67–72 (2006)
9. P. Blennow, A. Hagen, K.K. Hansen, L.R. Wallenberg, M. Mogensen, Solid State Ionics **179**, 2047–2058 (2008)
10. K. Ahn, S. Jung, J.M. Vohs, R.J. Gorte, Ceram Int **33**, 1065–1070 (2007)
11. Q. Ma, F. Tietz, D. Sebold, D. Stöver, J. Power, Sources **195**, 1920–1925 (2010)
12. X. Sun, S. Wang, Z. Wang, X. Ye, T. Wen, F. Huang, J. Power, Sources **183**, 114–117 (2008)
13. X. Sun, S. Wang, Z. Wang, J. Qian, T. Wen, F. Huang, J. Power, Sources **187**, 85–89 (2009)
14. S. Tao, J.T.S. Irvine, J Electrochem Soc **151**, A252–A259 (2004)
15. Ch Sun, U. Stimming, J. Power, Sources **171**, 247–260 (2007)
16. H. Kurokawa, L. Yang, C.P. Jacobson, L.C. De Jonghe, S.J. Visco, J. Power, Sources **164**, 510–518 (2007)
17. Q. Fu, F. Tietz, D. Sebold, S. Tao, J.T.S. Irvine, J. Power, Sources **171**, 663–669 (2007)